

Investigation of lattice-dynamical effects and hyperfine interactions in ZnO by ^{67}Zn Mössbauer spectroscopy

C. Schäfer, W. Potzel, W. Adlassnig, P. Pöttig, E. Ikonen,* and G. M. Kalvius

Physik-Department E15, Technische Universität München, D-8046 Garching, Federal Republic of Germany

(Received 26 May 1987; revised manuscript received 19 October 1987)

Using the high-resolution 93.3-keV transition in ^{67}Zn we studied the temperature dependence of the Lamb-Mössbauer factor (LMF), the center shift, and the quadrupole interaction in ZnO single crystals. The temperature range for this high-energy Mössbauer resonance could be extended up to liquid-nitrogen temperature (77.3 K). The mean-square atomic displacements show very little anisotropy. The results on the LMF can well be described by the Debye model with $\Theta_D^{\text{LMF}} \sim 317$ K. The quadrupole interaction is $e^2qQ/h = 2.401 \pm 0.004$ MHz at 4.2 K and it is independent of temperature within 1%. At 77.3 K the center shift has changed by $9.0 \mu\text{m/s}$ compared to its value at 4.2 K. Already at low temperatures, phonon-induced electron transfer from zinc to oxygen is observed. The shift caused by charge transfer shows a T^4 dependence at low temperatures, in agreement with theoretical calculations.

I. INTRODUCTION

The 93.3-keV transition in ^{67}Zn offers extremely high resolution for the determination of small changes in energy.¹⁻³ This exceptionally high sensitivity has thus far been used primarily for precision measurements of hyperfine interactions. Only recently it has been demonstrated that the ^{67}Zn Mössbauer resonance is also highly sensitive for studying lattice-dynamical effects.⁴⁻⁶ This sensitivity is due to the relatively large transition energy and the light mass of the Mössbauer atom. Of specific interest have been investigations of the temperature dependence of the second-order Doppler shift and of the anisotropy of the recoil-free fraction in zinc metal.^{4,5} Together with specific-heat data the Mössbauer results give information on the phonon frequency spectrum.

In the present paper we report on Mössbauer experiments performed with single crystals of ZnO. This material crystallizes in a hexagonal (wurtzite) structure and has the interesting feature that the thermal expansion coefficient is negative in the temperature range between 4 and ~ 100 K.^{7,8} Through refinements of the experimental techniques we were able to extend the measuring temperature upwards to 80 K despite the small Lamb-Mössbauer factor caused by the relatively high γ -ray energy and low mass of the resonant nucleus. Therefore we could derive mean-square atomic displacements for ^{67}Zn in the temperature range between 4 and 80 K. From a detailed analysis of the center shift we conclude that phonon-induced charge transfer from zinc to oxygen plays an important role. At low temperatures this charge transfer shows a T^4 dependence as predicted theoretically by Shrivastava.⁹ This is the first time that a T^4 dependence of the charge transfer has been observed experimentally. In addition, the temperature dependence of the electric-field gradient in ZnO was determined with high precision. All these measurements were performed as supplementary investigations within a series of experiments aiming at a determination of the red shift of γ

rays^{10,11} due to the gravitational field of the Earth with the ^{67}Zn resonance.

II. EXPERIMENTAL DETAILS

Measurements were performed in standard transmission geometry with a piezoelectric quartz spectrometer as described earlier.⁵ The drive system which is a compact unit containing both source and absorber was suspended by soft springs inside a sealed stainless-steel container filled with He exchange gas at reduced pressure.⁵ The temperature of the ZnO single-crystal source could be increased by a small heating coil. In this manner it was possible to keep the absorber temperature below 12 K even at a source temperature of 80 K. The temperatures of source and absorber were determined by semiconductor devices.

As a result of the small recoil-free fraction at higher temperatures experiments become increasingly difficult, in particular at liquid-nitrogen temperature. One could argue that it would be advantageous to heat the absorber rather than the source and compensate the smaller recoil-free fraction at elevated temperatures by increasing the absorber thickness. This, however, cannot be done here, since the electronic (photoelectric) absorption cross section is the factor limiting absorber thickness.^{3,11} The problem can only be overcome by using strong radioactive sources and fast-counting electronics, i.e., by measuring small resonance-absorption effects with high-statistical accuracy. In addition, in order to study the temperature dependence of anisotropic effects, one would have to grow single crystals enriched in ^{67}Zn which would be very costly.

The ^{67}Ga ($T_{1/2} = 78$ h) activity was produced *in situ* by 28-MeV proton bombardment of ZnO single crystals at the cyclotron of the Kernforschungszentrum Karlsruhe. The ZnO single crystals were disks of 4-mm diameter and of 0.5-mm thickness. They were cut with the c axis perpendicular to the crystal faces. After irradiation the samples were annealed in oxygen atmosphere at ~ 970 K for

6 h and thereafter slowly cooled (50 K/h) to room temperature. Mössbauer spectra were recorded with the c axis at 0° and 45° with respect to the direction of observation of the γ rays.

The absorber consisted of ^{67}ZnO powder, enriched to 85.2 wt.% in ^{67}Zn . The thickness was $963 \text{ mg } ^{67}\text{Zn}/\text{cm}^2$. Details of the absorber preparation are given elsewhere.¹²

The spectrometer was calibrated using the known quadrupole splittings in ^{67}Zn metal^{2,13} and in ^{67}ZnO (Refs. 1 and 2) at 4.2 K. The γ rays were detected by an intrinsic Ge diode of 10-mm thickness and 40-mm diameter coupled to a fast preamplifier. In order to achieve high-counting speed and simultaneously good energy resolution a fast double-differentiating main amplifier was used.¹⁴ Count rates up to $200\,000 \text{ s}^{-1}$ in the 93.3-keV window were obtained. The signal-to-noise ratio was determined once a day by recording pulse-height spectra at the actual counting rate via a high-speed analog-to-

digital converter. Typical values for the signal-to-noise ratio were 60–70 %.

III. RESULTS

A. Lamb-Mössbauer factor

Figures 1 and 2 display Mössbauer absorption spectra recorded at source temperatures between 4.2 and 77.3 K for orientations of the ZnO single crystal of $\theta=0^\circ$ and 45° of the c axis with respect to the direction of observation of the 93.3-keV γ rays. The spectra were least-squares fitted to a superposition of five (respectively, seven) independent Gaussian lines. The results are summarized in Tables I and II. The linewidths observed are substantially above the natural width. The cause for this broadening are random vibrations originating in the boiling helium. Therefore the overall line shape could not be well represented by a Lorentzian and hence we have chosen a Gaussian line profile for the fit.

The Lamb-Mössbauer factor and the mean-square atomic displacements are derived from the total area under the absorption lines after correction for nonresonant background radiation. In addition, a value of $f_{\parallel}=(2.03\pm 0.12)\%$ was used for the recoil-free fraction in ZnO single crystals at 4.2 K with $\theta=0^\circ$. This value is

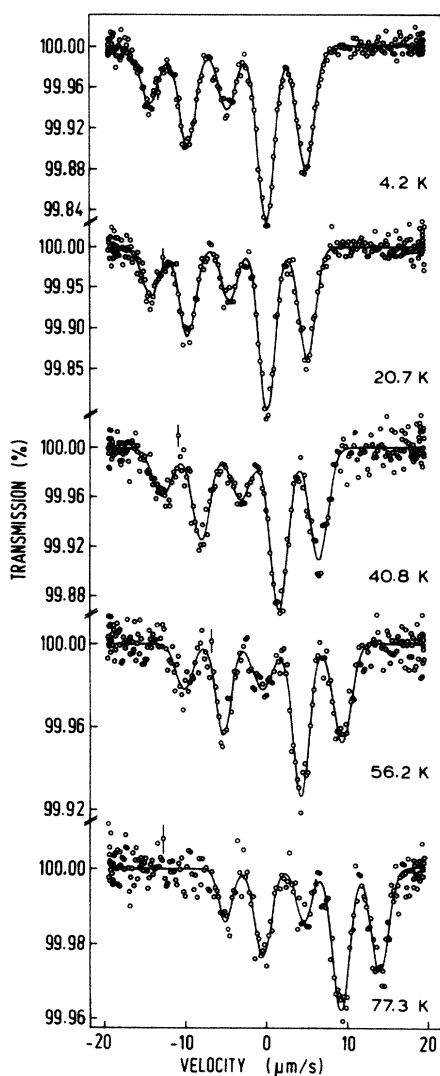


FIG. 1. Mössbauer absorption spectra recorded at source temperatures between 4.2 and 77.3 K. The source is a $^{67}\text{GaZnO}$ single crystal with the c axis parallel to the direction of observation of the 93.3-keV γ rays.

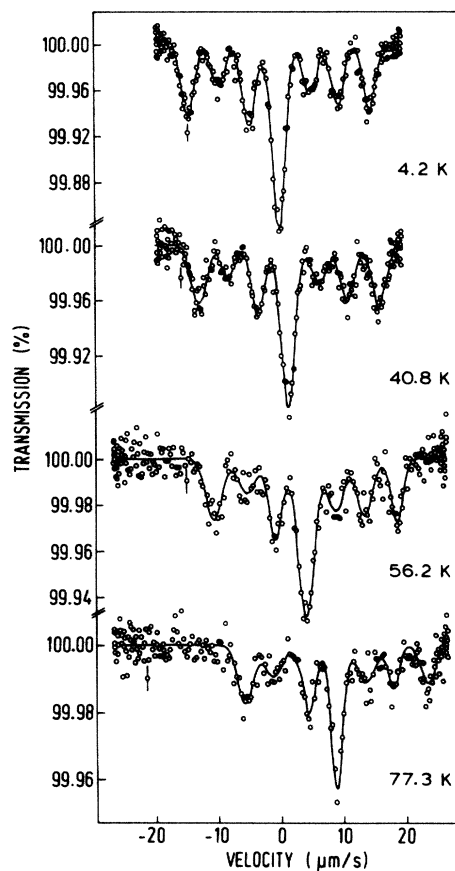


FIG. 2. Mössbauer absorption spectra obtained at source temperatures between 4.2 and 77.3 K. The c axis of the $^{67}\text{GaZnO}$ single crystal forms an angle of 45° with respect to the direction of observation of the 93.3-keV γ rays.

TABLE I. Summary of measured Mössbauer parameters at various temperatures for ZnO single crystal with c axis parallel to the direction of observation of the 93.3 keV γ rays. Only statistical errors are quoted.

T (K)	Area (% $\mu\text{m/s}$)	Linewidth ($\mu\text{m/s}$)	Position ($\mu\text{m/s}$)	Total area (% $\mu\text{m/s}$)	Center shift ($\mu\text{m/s}$)
4.2	0.147(7)	2.6(1)	-14.21(6)	1.29(2)	0.04(2)
	0.246(8)	2.52(9)	-9.64(4)		
	0.164(8)	2.6(2)	-4.75(6)		
	0.423(8)	2.46(5)	0.02(2)		
	0.313(8)	2.60(7)	4.89(3)		
20.7	0.15(1)	2.5(2)	-14.10(8)	1.37(3)	0.08(3)
	0.26(1)	2.4(1)	-9.64(5)		
	0.16(1)	2.3(2)	-4.53(8)		
	0.46(1)	2.28(7)	0.10(3)		
	0.33(1)	2.4(1)	4.99(4)		
40.8	0.12(1)	3.0(3)	-12.7(1)	1.02(3)	1.55(3)
	0.19(1)	2.5(2)	-7.96(7)		
	0.13(1)	3.1(4)	-3.1(1)		
	0.34(1)	2.5(1)	1.56(4)		
	0.24(1)	2.6(1)	6.39(6)		
56.2	0.054(7)	2.5(4)	-10.0(1)	0.50(2)	4.28(4)
	0.092(7)	2.1(2)	-5.25(7)		
	0.061(8)	2.8(4)	-0.4(2)		
	0.173(7)	2.3(1)	4.24(5)		
	0.122(7)	2.6(2)	9.25(7)		
77.3	0.029(4)	2.0(3)	-5.1(1)	0.279(9)	9.08(4)
	0.057(4)	2.4(2)	-0.43(9)		
	0.032(4)	2.3(3)	4.6(1)		
	0.092(4)	2.4(1)	9.12(5)		
	0.070(4)	2.5(2)	13.85(6)		

the average of the results obtained by two earlier experiments.^{12,15}

The angular dependence of the recoil-free fraction $f(\theta)$ for an axially symmetric lattice is given by

$$f(\theta) = \exp\{-\mathbf{k}^2[\langle x_{\text{Zn}}^2 \rangle_{\perp} + (\langle x_{\text{Zn}}^2 \rangle_{\parallel} - \langle x_{\text{Zn}}^2 \rangle_{\perp}) \cos^2 \theta]\}, \quad (1)$$

where \mathbf{k} is the wave vector of the γ radiation and $\langle x_{\text{Zn}}^2 \rangle_{\perp}$ and $\langle x_{\text{Zn}}^2 \rangle_{\parallel}$ denote the mean-square atomic displacements of ^{67}Zn perpendicular and parallel to the c axis, respectively. Table III gives the results together with the corresponding Lamb-Mössbauer factors f_{\perp} and f_{\parallel} . Above ~ 50 K the values for $\langle x_{\text{Zn}}^2 \rangle_{\parallel}$ tend to be larger than those for $\langle x_{\text{Zn}}^2 \rangle_{\perp}$, however, just outside our present limits of error. If at all, there is very little anisotropy of the mean-square atomic displacements at low temperature.

B. Center shift

A change with temperature of the center shift is clearly visible in Figs. 1 and 2. At 77.3 K it has increased to a value of $+9.01 \pm 0.03 \mu\text{m/s}$ as compared to 4.2 K (see

Tables I and II). At low temperatures our data for the center shift S_C show a T^4 dependence:

$$S_C(T_S) - S_C(T_A) = \alpha(T_A^4 - T_S^4), \quad (2)$$

where T_S and T_A are the temperatures of source and absorber, respectively, and α is a constant. From our Mössbauer experiments we get $\alpha_M = 5.7 \pm 0.3 \times 10^{-7} \mu\text{m s}^{-1} \text{K}^{-4}$. This value is at variance with an earlier but less precise Mössbauer experiment,¹⁶ which gave only $4.2 \times 10^{-7} \mu\text{m s}^{-1} \text{K}^{-4}$.

As will be discussed below, the center shift is due to the second-order Doppler shift¹⁷ and to the explicit temperature dependence of the isomer shift which is significant surprisingly even at temperatures as low as 20 K.

C. Quadrupole interaction

Due to the hexagonal structure of ZnO an electric-field gradient is present at the Zn nucleus both in the source as well as in the absorber. If $\theta = 0^\circ$, the quadrupole interaction in the source leads to relative intensities of the emitted lines of 0:2:1 (Ref. 18), whereas at $\theta = 45^\circ$ we have

TABLE II. Summary of measured Mössbauer parameters at various temperatures for ZnO single crystal with orientation of $\theta=45^\circ$ of the c axis with respect to the direction of observation of the 93.3 keV γ rays. Only statistical errors are quoted.

T (K)	Area (% $\mu\text{m/s}$)	Linewidth ($\mu\text{m/s}$)	Position ($\mu\text{m/s}$)	Total area (% $\mu\text{m/s}$)	Center shift ($\mu\text{m/s}$)
4.2	0.157(8)	2.5(1)	-14.28(5)	1.21(2)	-0.02(4)
	0.094(8)	2.5(2)	-9.46(9)		
	0.179(9)	2.5(1)	-4.67(6)		
	0.399(9)	2.50(6)	-0.01(3)		
	0.111(9)	2.5(2)	4.89(9)		
	0.126(8)	2.4(2)	9.34(7)		
	0.141(8)	2.5(1)	14.32(5)		
40.8	0.121(9)	2.8(2)	-12.67(8)	0.91(2)	1.42(4)
	0.057(8)	2.4(4)	-8.1(2)		
	0.124(9)	2.5(2)	-3.35(8)		
	0.301(9)	2.56(9)	1.38(3)		
	0.077(9)	2.8(4)	6.3(2)		
	0.107(9)	2.6(3)	10.7(1)		
	0.127(8)	2.8(2)	15.68(7)		
56.2	0.082(8)	3.1(4)	-10.5(1)	0.64(2)	4.09(6)
	0.05(1)	3.2(8)	-5.3(3)		
	0.090(9)	2.5(3)	-0.7(1)		
	0.21(1)	3.1(2)	4.10(6)		
	0.07(1)	3.1(6)	8.9(2)		
	0.072(9)	2.8(4)	13.4(2)		
	0.067(6)	2.4(3)	18.4(1)		
	0.051(7)	2.9(4)	-5.6(2)	0.33(2)	8.89(5)
	0.031(7)	3.2(9)	-1.1(3)		
	0.053(5)	2.6(3)	4.4(1)		
	0.093(5)	2.2(1)	8.87(5)		
	0.040(7)	3.5(7)	13.5(2)		
	0.027(4)	2.1(4)	17.9(2)		
	0.032(4)	2.8(4)	23.2(2)		

three lines with relative intensities of 1.36:1:2. The quadrupole interaction in the ZnO powder absorber gives three absorption transitions of equal intensities. Thus the absorption spectra with $\theta=0^\circ$ exhibit five peaks with relative intensities of 1:2:1:3:2 and those with $\theta=45^\circ$ have seven peaks with relative intensities of 2:1:2:4.36:1:1.36:1.36 (see Figs. 1 and 2). When calculating these relative intensities it was assumed that the anisotropy of the mean-square atomic displacements is negligible. The main component of the quadrupole tensor and the asymmetry parameter η were derived from the line separations.² As can be seen by Tables I and II and Fig. 3 the change of the quadrupole interaction with temperature up to 77.3 K is smaller than 1%. We get

$$e^2qQ/h = 2.401 \pm 0.004 \text{ MHz}$$

at 4.2 K and for the ratio

$$e^2qQ(4.2 \text{ K})/e^2qQ(77.3 \text{ K}) = 1.009 \pm 0.010 .$$

Within our experimental errors the asymmetry parameter is found to be $\eta=0$ at all temperatures.

IV. DISCUSSION

A. Lamb-Mössbauer factor

1. Mean-square atomic displacements for zinc

Within our present limits of error there is very little anisotropy of the recoil-free fraction (see Table III). This is in perfect accordance with the similarity of the Grüneisen parameters γ_{\parallel} and γ_{\perp} deduced from thermal-expansion coefficients and related data,^{7,8} which implies that the elastic anisotropy of the crystal must be small. This result is in sharp contrast to the situation in Zn metal, where an enormously large anisotropy was found.^{4,5} In Fig. 4 the mean-square atomic displacements $\langle x_{\text{Zn}}^2 \rangle_{\perp}$ and $\langle x_{\text{Zn}}^2 \rangle_{\parallel}$ for Zn atoms are plotted versus temperature. The solid lines are fits by the Debye model with effective Debye temperatures of $\Theta_D^{\text{LMF}} = 319 \pm 6 \text{ K}$ and $315 \pm 5 \text{ K}$, respectively. The Debye model fits the data points quite well indeed.

In hexagonal ZnO each Zn atom is surrounded by four oxygen atoms arranged in a slightly distorted tetrahedron. The nearly isotropic Lamb-Mössbauer factor indi-

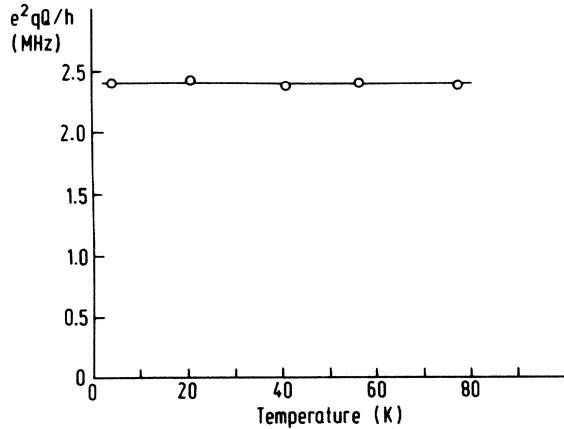


FIG. 3. Quadrupole interaction in ^{67}ZnO at various temperatures. The change of e^2qQ/h between 4.2 and 77.3 K is smaller than 1%.

cates that the chemical bonds to the four oxygens are almost equal. This is further corroborated by the relatively small quadrupole interaction (see below).

2. Mean-square atomic displacements for oxygen

In the limit $T \rightarrow 0$, mean-square atomic displacements can also be derived for the oxygen atoms. Since the anisotropy is very small, we take $\langle x^2 \rangle_{\perp} = \langle x^2 \rangle_{\parallel} = \langle x^2 \rangle$. Then the following relation is valid for $T \rightarrow 0$ (Ref. 19):

$$3(2M_{\text{Zn}} \langle x_{\text{Zn}}^2 \rangle + 2M_{\text{O}} \langle x_{\text{O}}^2 \rangle) = 3N\hbar/\omega(-1), \quad (3)$$

where M_{Zn} and M_{O} are the gram atomic weights for Zn and O, respectively, and $3N$ is the total number of degrees of freedom. The (-1) st moment $\omega(-1)$ of the phonon frequency distribution can be determined from specific-heat measurements.⁸ Taking $\omega(-1)$ from Ref. 8 we derive $\langle x_{\text{O}}^2 \rangle / \langle x_{\text{Zn}}^2 \rangle = 2.2 \pm 0.3$. For small mass changes, $\langle x_k^2 \rangle$ (for atom k) is expected to be approximately proportional to $M_k^{-1/2}$ and approximately independent of the other masses.¹⁹ Our result indicates that this approximation is well fulfilled for ZnO, although the masses of Zn and O differ by more than a factor of 4.

TABLE III. Lamb-Mössbauer factors f_{\parallel} and f_{\perp} , parallel and perpendicular to the c axis of ZnO, respectively, and corresponding mean-square atomic displacements $\langle x_{\text{Zn}}^2 \rangle$ obtained at various temperatures. The errors quoted include the statistical errors, a 2% uncertainty in the determination of the signal-to-noise ratio in the γ -ray spectrum and an error of 6% in the value for f_{\parallel} at 4.2 K.

T (K)	f_{\parallel} (%)	$\langle x_{\text{Zn}}^2 \rangle_{\parallel}$ (\AA^2)	f_{\perp} (%)	$\langle x_{\text{Zn}}^2 \rangle_{\perp}$ (\AA^2)
4.2	2.03(12)	0.001 74(3)	2.06(21)	0.001 74(4)
20.7	2.00(14)	0.001 75(4)	not measured	
40.8	1.48(10)	0.001 88(4)	1.42(15)	0.001 90(5)
56.2	0.80(6)	0.002 16(4)	1.24(13)	0.001 96(5)
77.3	0.44(3)	0.002 43(4)	0.64(7)	0.002 26(5)

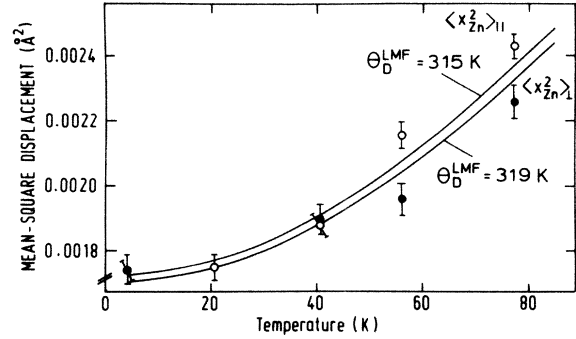


FIG. 4. Mean-square atomic displacements of ^{67}Zn in ZnO, parallel and perpendicular to the c axis. The solid lines are fits by the Debye model with Debye temperatures of $\Theta_D^{\text{LMF}} = 315$ and 319 K, respectively.

B. Center shift

The temperature variation of the center shift S_C can be written:^{20,21}

$$\begin{aligned} (\partial S_C / \partial T)_p = & (\partial S_{\text{SOD}} / \partial T)_p + (\partial S / \partial T)_V \\ & + (\partial S / \partial \ln V)_T (\partial \ln V / \partial T)_p. \end{aligned} \quad (4)$$

The first term represents the second-order Doppler shift (SOD). The second term describes the explicit temperature dependence of the isomer shift S at constant volume due to changes of the electron density which may be caused by the electron-phonon interaction upon the electronic states. The third term gives the volume dependence of S caused by thermal expansion of the lattice. Although there are no high-pressure Mössbauer data on ZnO available at present, the contribution of the third term to the center shift can be estimated to be negligibly small. The total-volume contraction between 4.2 K and 80 K is smaller than 1×10^{-4} .^{7,8} The s -electron density ρ is calculated for $^{67}\text{Zn}^{2+}$ in a tetrahedral environment of O^{2-} ions to vary proportional to the inverse seventh power of interatomic distance R (Ref. 22), i.e., $\Delta\rho \simeq -(\frac{2}{3})(\Delta V/V)\rho$ with $\rho \sim 7.5$ a.u. for $R \sim 2 \text{ \AA}$.²³ Together with the known value of $\Delta\langle r^2 \rangle$ (Refs. 24 and 25) we estimate $\Delta S \sim 0.8 \mu\text{m/s}$, or only $\sim 0.8\%$ of the center shift observed between 4.2 and 77 K. Thus, to a very good approximation, the center shift is due to the second-order Doppler shift (S_{SOD}) and the explicit temperature dependence of the isomer shift (S_{ET}).

The main problem is the separation of the S_{SOD} from the center shift.¹⁹ We attempt to achieve this by using specific heat data C_p .²⁶⁻²⁸ Since the volume change is rather small up to $T \sim 100$ K the specific heat C_V can very well be approximated by the experimental data C_p in this temperature range. As demonstrated by Fig. 5 the change in specific heat C_V follows closely the curve calculated within the Debye model if a Debye temperature of $\Theta_D^{\text{sp}} = 275 \pm 3$ K is chosen and the assumption is made that only acoustic phonons play a role at low temperatures. When these low-frequency phonons are excited, the whole ZnO molecule moves together. Optical-phonon

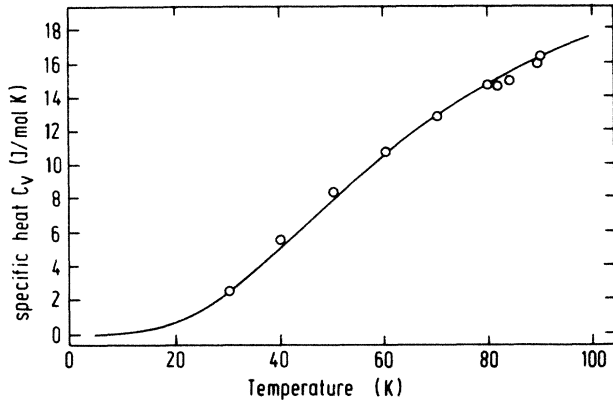


FIG. 5. Specific heat of ZnO within the temperature range covered by the Mössbauer experiments. The best fit by the Debye model in the temperature range ($T \lesssim 100$ K) gives a Debye temperature of $\Theta_D^{\text{sp}} = 275$ K. The specific-heat data are taken from Refs. 26–28.

frequencies appear to lie much higher indeed.

When the temperature of a harmonic crystal is increased, the change of the total energy is twice the change of the mean kinetic energy:

$$M_{\text{Zn}} \Delta \langle v_{\text{Zn}}^2 \rangle + M_{\text{O}} \Delta \langle v_{\text{O}}^2 \rangle = \Delta E, \quad (5)$$

where E is the total energy of the lattice, and $\langle v_{\text{Zn}}^2 \rangle$, and $\langle v_{\text{O}}^2 \rangle$ are the mean-square atomic velocities of Zn and O, respectively.

We consider, respectively, the two limiting cases of high and low temperatures. At *high* temperatures in thermodynamic equilibrium the mean kinetic energies for Zn and O change by equal amounts. Then Eq. (5) reduces to

$$\Delta \langle v_{\text{Zn}}^2 \rangle = 1/(2M_{\text{Zn}}) \Delta E. \quad (6)$$

Therefore in ZnO at high temperatures the second-order Doppler shift $S_{\text{SOD}} = -\Delta \langle v^2 \rangle / (2c)$ is connected to the specific heat by:

$$S_{\text{SOD}} = -\Delta T C_V / (4M_{\text{Zn}} c), \quad (7)$$

where c is the velocity of light and ΔT is the difference in temperature. The line shift S_{SOD} can therefore be predicted by integrating Eq. (7) with known specific heat. The dashed line labeled S_{SOD}^H in Fig. 6 indicates the temperature dependence of the second-order Doppler shift as calculated from the specific heat, if the assumption would be valid that Eq. (7) also holds at low temperature.

In the second limiting case of *low* temperatures, the change of $\langle v^2 \rangle$ between 0 K and temperature T is given by:¹⁹

$$\langle v^2 \rangle_T - \langle v^2 \rangle_{T=0} = (3\pi^4/5)(k_B/M)\theta_0(T/\theta_0)^4, \quad (8)$$

where k_B is the Boltzmann constant.

At low temperatures this increase in $\langle v^2 \rangle$ is the same for zinc and oxygen, although the absolute values are different. This increase is caused by the very long-wavelength acoustic vibrations which are the first to be

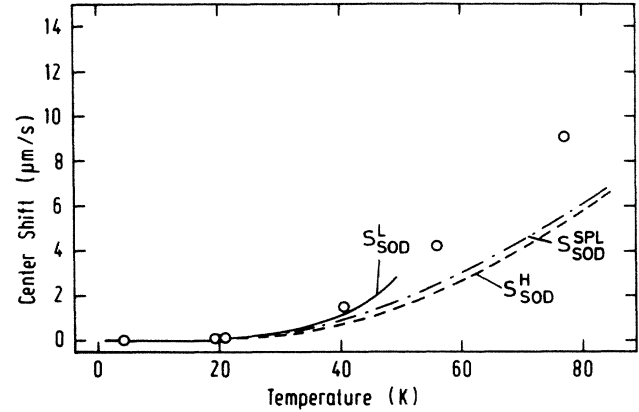


FIG. 6. Center shift at various temperatures. The error bars are smaller than the open circles representing the data points (Ref. 29). S_{SOD}^L and S_{SOD}^H correspond to the second-order Doppler shift as calculated from specific-heat data for the low- and high-temperature limit, respectively. $S_{\text{SOD}}^{\text{spl}}$ denotes the second-order Doppler shift as calculated from a spline interpolation between the low- and high-temperature limits (see text).

excited. Since in these modes groups of atoms move together, the motion of a particular atom does not depend on its mass, force constants, or local surroundings, but only on the bulk elastic constants of the crystal. In Eq. (8) M is the mass of a ZnO molecule. The value of θ_0 is obtained by fitting a T^3 dependence to the *low*-temperature specific-heat data with the condition that the total number of modes allowed is 3 times the number of ZnO molecules. The curve labeled S_{SOD}^L in Fig. 6 is calculated using Eq. (8) with $\theta_0 = 275$ K. Up to ~ 50 K S_{SOD}^L lies considerably below the data points obtained experimentally for S_C (see Fig. 6). This is true also for the value at 19.4 K, where $S_{\text{SOD}}^L = 0.066 \pm 0.002$ $\mu\text{m/s}$ and $S_C = 0.080 \pm 0.003$ $\mu\text{m/s}$. The fact that the observed S_C is larger than both S_{SOD}^H and S_{SOD}^L demonstrates that the explicit temperature-dependent isomer shift plays a decisive role already at cryogenic temperatures.

In order to determine the S_{ET} quantitatively, the derivation of the S_{SOD} for the zinc atoms at intermediate temperatures is needed. This is a formidable task. It requires modern cluster calculations, which in particular allow a determination of force constants. At present such calculations are not available. However, using Eqs. (7) and (8) as a basis we can say that the S_{ET} has to be within a certain region: It has to be at least as large as the difference between the experimental values for S_C and the curve S_{SOD}^L (i.e., $S_{\text{ET}} \geq S_{\text{ET,min}}$), and it has to be smaller than the difference between S_C and the curve S_{SOD}^H (i.e., $S_{\text{ET}} \leq S_{\text{ET,max}}$). Furthermore, S_{ET} has to approach $S_{\text{ET,min}}$ at low temperatures and $S_{\text{ET,max}}$ at high temperatures. To get a more quantitative estimate we took $S_{\text{SOD}} = S_{\text{SOD}}^L$ at 19.4 K and $S_{\text{SOD}} = S_{\text{SOD}}^H$ at 297.9 K (the highest temperature for which specific-heat data are available) and used a spline interpolation for the temperature range in between. This spline curve $S_{\text{SOD}}^{\text{spl}}$ is also shown in Fig. 6. The S_{ET} is then given as difference between S_C and the spline curve. Table IV summarizes the

TABLE IV. Center shift (S_C), explicit temperature-dependent isomer shift (S_{ET}), calculated as difference between center shift (S_C) and second-order Doppler shift (S_{SOD}^{sp}) as described in the text. Theoretical values are calculated from Eq. (9) using a charge-transfer model.

Temperature (K)	S_C ($\mu\text{m/s}$)	S_{ET} ($\mu\text{m/s}$)	Charge-transfer model ($\mu\text{m/s}$)
19.4	0.080 ± 0.003	0.014 ± 0.005	0.028
20.7	0.08 ± 0.03	0.00 ± 0.04	0.036
40.8	1.50 ± 0.03	0.49 ± 0.06	0.50
56.2	4.22 ± 0.04	1.7 ± 0.2	1.45
77.3	9.01 ± 0.03	3.5 ± 0.3	3.58

derived values for the S_{ET} at various temperatures. In Fig. 7 the S_{ET} is plotted versus temperature.

The change of S_{ET} is such, that the s -electron density $\rho(0)$ at the Zn nucleus is *reduced* with increasing temperature. Anharmonic effects, like lattice contraction, cannot explain the observed S_{ET} . As estimated above, the shift caused by lattice contraction is about a factor of 50 smaller than S_{ET} . In addition, lattice contraction is expected to increase $\rho(0)$ due to the larger covalency of the Zn-O bond.²⁴ Therefore our data clearly demonstrate the presence of S_{ET} . Most likely it is caused by phonon-induced processes which involve the electronic structure.

Changes in the s -electron density at the Mössbauer nucleus as a result of the electron-phonon interaction have been calculated^{9,30-32} and experimentally investigated in some conducting^{21,33-35} as well as insulating systems.^{36,37} In all cases, phonon-induced effects have been observed only at high temperatures, where, however, other effects, like thermal expansion, are large. In ZnO the electron-phonon interaction appears to be important already at cryogenic temperatures.

Shrivastava has theoretically investigated two types of phonon-induced processes for the case of ⁵⁷Fe: dynamical

configuration mixing and dynamical charge transfer.⁹ In ZnO dynamical configuration mixing can be neglected, since the $3d$ shell of Zn is completely filled and the $4d$ levels lie energetically too high to be involved in the chemical bond. Dynamical charge transfer, however, appears to play the important role. As stated earlier,^{24,38} the chemical bond in ZnO is partially covalent. The dynamical phonon-induced electron transfer from partially occupied $4s$ and $4p$ orbitals of zinc to the neighboring oxygen atoms is mediated by the orbital-lattice interaction. Such an electron transfer indeed decreases the s -electron density $\rho(0)$ at the zinc nucleus. From our measured value of $\sim 3.5 \mu\text{m/s}$ (at 77.3 K) we estimate a charge transfer which corresponds to a fraction of 0.01 of a $4s$ electron.

The temperature dependence of the dynamical charge transfer was predicted⁹ to cause S_{ET} to vary according to

$$S_{ET} = KT^4\Phi(T), \quad (9)$$

where K is a constant containing the electronic matrix elements. In Ref. 9 the Debye approximation was used with

$$\Phi(T) = \int_0^{\Theta/T} z^3 (e^z - 1)^{-1} dz, \quad (10)$$

where Θ is an effective Debye temperature.

From our measurements we derive $K = 3.0 \pm 1.0 \times 10^{-8} \mu\text{m s}^{-1} \text{K}^{-4}$ and $\Theta = 275 \pm 3 \text{ K}$. The relatively large error in the value for K is mainly due to the uncertainty in the spline interpolation. The solid line in Fig. 7 is calculated with these parameters. The values are also summarized in Table IV. Considering the relatively simple spline interpolation, the agreement with our experimental data is very good. In addition, the value of Θ agrees perfectly with the Debye temperature Θ_D^{sp} derived from specific-heat data in this temperature range. At low temperatures $\Phi(T)$ is temperature independent to good approximation [if $(\Theta/T) > 7$, the deviation of $\Phi(T)$ from $\Phi(0) = \pi^4/15$ is less than 5%]. Therefore

$$S_{ET} = K(\pi^4/15)T^4. \quad (11)$$

Although the change of the s -electron density at the ⁶⁷Zn nucleus is exceedingly small, the high-resolution spectroscopy of the 93.3 keV transition makes it possible to determine phonon-induced charge transfer with high

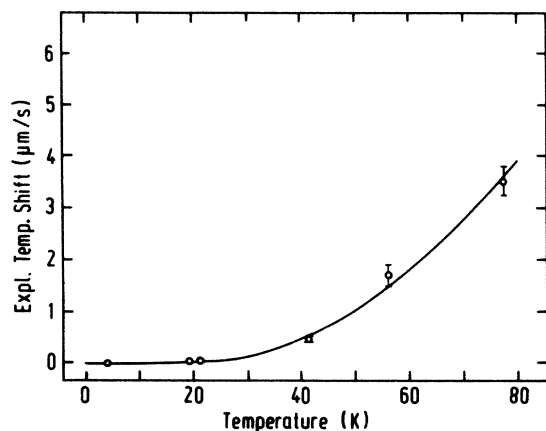


FIG. 7. Explicit temperature dependence of the isomer shift (S_{ET}). S_{ET} is the difference between S_C and S_{SOD}^{sp} of Fig. 6. The solid line is a fit to the data using the equation $S_{ET} = KT^4\Phi(T)$. At low temperatures a T^4 dependence is observed.

precision. Unfortunately, for ^{67}Zn systems calculations, in particular of the constant K , are still missing.

One might argue that the second-order Doppler shift $S_{\text{SOD}} = -\Delta\langle v^2 \rangle / (2c)$ does not cover the total center shift, because it has implicitly been assumed that accelerations of the atoms due to lattice vibrations do not cause an extra energy shift of the γ radiation.³⁹ The accelerations involved are extremely large, of the order of 10^{16} ms^{-2} . The difference between S_C and S_{SOD} observed in our experiments gives an upper limit for such an effect: The change of γ frequency produced by these accelerations is smaller than one part in 10^{14} .

C. Quadrupole interaction

As demonstrated by Tables I, II, and Fig. 3 the electric-field gradient tensor (efg) is independent of temperature between 4.2 and 77.3 K within $\sim 1 \times 10^{-2}$. A NMR measurement⁴⁰ on a single crystal of ZnO at room temperature gave $e^2qQ/h = 2.409 \pm 0.010$ MHz. This implies that the efg would change very little indeed, even up to room temperature. Our data on ZnO are further corroborated by time-differential perturbed-angular correlation (TDPAC) measurements using, however, the probe ^{111}Cd as an impurity in ZnO.^{41,42} The TDPAC results exhibit very little change up to ~ 70 K, a slow decrease of the quadrupole interaction up to ~ 300 K and an exponential increase above ~ 400 K. In addition, the TDPAC data show a reduction of the quadrupole coupling constant at low temperatures by $\sim 1\%$ in ZnO single crystals as compared to ZnO powder. This reduction should also be visible in our Mössbauer data. With our measurements we find a small but systematic difference between S_C for $\theta = 0^\circ$ and for $\theta = 45^\circ$ (see Tables I and II). This is an indication for a slightly smaller efg in ZnO single crystals as compared to ZnO powder. However, in order to determine this difference more precisely, we have to improve the statistical accuracy of our measurements as well as the temperature stability of our experimental setup.

Neither the TDPAC nor the Mössbauer results are fully understood at present. The electric-field gradient can surprisingly be well described within a point-charge model⁴³ assuming complete ionicity in ZnO (i.e., Zn^{2+} and O^{2-}). The point-charge model predicts a temperature independent efg if the change caused by a lattice contraction parallel to the c axis is compensated by the change due to the lattice contraction perpendicular to the c axis. The application of the point charge model, however, has to be considered doubtful, since the chemical bond in

ZnO is partially covalent. As stated earlier,^{24,38} a clear indication of this fact is the much more negative isomer shift which was found for ZnF_2 . In fact, an investigation of the electric quadrupole interaction in ZnF_2 demonstrated that even this compound is not fully ionic.³⁸ The phonon-induced electron transfer from zinc to oxygen also stresses the partially covalent character of the Zn—O bond. Although the electron transfer decreases the charge at the zinc site, the symmetry of the charge distribution, which is reflected in the quadrupole interaction, remains virtually unchanged. An improvement of our understanding of the dynamical charge transfer process and of electric-field gradients and their temperature dependence requires highly detailed theoretical calculations.

V. CONCLUSIONS

The 93.3-keV transition in ^{67}ZnO was used to investigate the temperature dependence of the quadrupole interaction, the Lamb-Mössbauer factor, and the center shift. The quadrupole interaction is independent of temperature within 1% between 4.2 and 77 K. The mean-square atomic displacements were found to show very little anisotropy. Most interesting is the variation of the center shift with temperature. Already at low temperatures (~ 20 K) phonon-induced electron transfer from zinc to oxygen causes a significant contribution to the center shift. The shift due to charge transfer shows a T^4 dependence. The charge transfer amounts to only ~ 0.01 of a $4s$ electron at 77.3 K and decreases $\rho(0)$, the s -electron density at the ^{67}Zn nucleus. Although the change of $\rho(0)$ is exceedingly small, the high-energy resolution of the 93.3-keV transition makes it possible to determine such effects with high precision.

ACKNOWLEDGMENTS

We would like to thank Dr. H. Schweickert, K. Assmus, and W. Maier at the cyclotron of the Kernforschungszentrum Karlsruhe for the numerous source irradiations. We acknowledge most valuable discussions with W. Schiessl. One of us (E.I.) gratefully acknowledges the warm hospitality at the Physik-Department E15, Technische Universität München, and the financial support by the Deutscher Akademischer Austauschdienst. This work has been funded by the German Federal Minister for Research and Technology (BMFT) under Contract No. 03-KA1TUM-4 and by the Kernforschungszentrum Karlsruhe.

*Permanent address: Helsinki University of Technology, Department of Technical Physics, Finland.

¹G. J. Perlow, W. Potzel, R. M. Kash, and H. de Waard, *J. Phys. (Paris)* **35**, C6-197 (1974).

²W. Potzel, Th. Obenhuber, A. Forster, and G. M. Kalvius, *Hyperfine Interact.* **12**, 135 (1982).

³P. Helistö, E. Ikonen, T. Katila, W. Potzel, and K. Riski, *Phys. Rev. B* **30**, 2345 (1984).

⁴W. Potzel, U. Närger, Th. Obenhuber, J. Zänkert, W. Adlassnig, and G. M. Kalvius, *Phys. Lett.* **98A**, 295 (1983).

⁵W. Potzel, W. Adlassnig, U. Närger, Th. Obenhuber, K. Riski, and G. M. Kalvius, *Phys. Rev. B* **30**, 4980 (1984).

⁶Th. Obenhuber, W. Adlassnig, J. Zänkert, U. Närger, W. Potzel, and G. M. Kalvius, *Hyperfine Interact.* **33**, 69 (1987).

⁷H. Ibach, *Phys. Status Solidi* **33**, 257 (1969).

⁸B. Yates, R. F. Cooper, and M. M. Kreitman, *Phys. Rev. B* **4**,

- 1314 (1971).
- ⁹K. N. Shrivastava, *Hyperfine Interact.* **24-26**, 817 (1985).
- ¹⁰R. V. Pound and J. L. Snider, *Phys. Rev.* **140**, B788 (1965).
- ¹¹T. Katila and K. J. Riski, *Phys. Lett.* **83A**, 51 (1981).
- ¹²W. Potzel, A. Forster, and G. M. Kalvius, *J. Phys. (Paris)* **37**, C6-691 (1976).
- ¹³Th. Obenhuber, A. Forster, W. Potzel, and G. M. Kalvius, *Nucl. Instrum. Methods* **214**, 361 (1983).
- ¹⁴W. Potzel and N. Halder, *Nucl. Instrum. Methods* **226**, 418 (1984).
- ¹⁵E. Ikonen, P. Helistö, T. Katila, and K. Riski, *Phys. Rev. A* **32**, 2298 (1985).
- ¹⁶A. I. Beskrovni, N. A. Lebedev, and Yu. M. Ostanevich, in *Proceedings of the Conference on Mössbauer Spectroscopy*, edited by H. Schnorr and M. Kautz (Deutsche Akademie der Wissenschaften zu Berlin, Dresden, 1971).
- ¹⁷G. K. Shenoy, F. E. Wagner, and G. M. Kalvius, in *Mössbauer Isomer Shifts*, edited by G. K. Shenoy and F. E. Wagner (North-Holland, Amsterdam, 1978), p. 101.
- ¹⁸G. J. Perlow, L. E. Campbell, L. E. Conroy, and W. Potzel, *Phys. Rev. B* **7**, 4044 (1973).
- ¹⁹R. M. Housley and F. Hess, *Phys. Rev.* **146**, 517 (1966).
- ²⁰R. V. Pound, G. B. Benedek, and R. Drever, *Phys. Rev. Lett.* **7**, 405 (1961).
- ²¹G. M. Rothberg, S. Guimard, and N. Benczer-Koller, *Phys. Rev. B* **1**, 136 (1970).
- ²²K. N. Shrivastava, *Phys. Rev. B* **13**, 2782 (1976).
- ²³S. C. Abrahams and J. L. Bernstein, *Acta Crystallogr.* **B25** 1233 (1969).
- ²⁴A. Forster, W. Potzel, and G. M. Kalvius, *Z. Phys. B* **37**, 209 (1980).
- ²⁵A. Svane and E. Antoncik, *Phys. Rev. B* **33**, 7462 (1986).
- ²⁶Y. S. Touloukian and E. H. Buyco, *Thermophysical Properties of Matter* (Plenum, New York, 1970), Vol. 5, p. 290.
- ²⁷K. Clusius and P. Harteck, *Z. Phys. Chem.* **134**, 243 (1928).
- ²⁸R. W. Millar, *J. Am. Chem. Soc.* **50**, 2653 (1928).
- ²⁹The data point shown at 19.4 K in Figs. 6 and 7 was obtained with a powdered sample of ZnO in a supplementary experiment. The agreement with the single-crystal data is excellent.
- ³⁰R. V. Kasowski and L. M. Falicov, *Phys. Rev. Lett.* **22**, 1001 (1969).
- ³¹K. N. Shrivastava, *Phys. Rev. B* **1**, 955 (1970).
- ³²K. N. Shrivastava, *Phys. Rev. B* **7**, 921 (1973).
- ³³R. M. Housley and F. Hess, *Phys. Rev.* **164**, 340 (1967).
- ³⁴D. L. Williamson, in *Mössbauer Isomer Shifts*, Ref. 17.
- ³⁵G. Kaindl, D. Salomon, and G. Wortmann, in *Mössbauer Isomer Shifts*, Ref. 17.
- ³⁶G. M. Kalvius, U. F. Klein, and G. Wortmann, *J. Phys. (Paris)* **35**, C6-139 (1974), and references therein.
- ³⁷H. K. Perkins and Y. Hazony, *Phys. Rev. B* **5**, 7 (1972).
- ³⁸W. Potzel and G. M. Kalvius, *Phys. Lett.* **110A**, 165 (1985).
- ³⁹T. E. Cranshaw, B. W. Dale, G. O. Longworth, and C. E. Johnson, *Mössbauer Spectroscopy and Its Applications* (Cambridge University, Cambridge, 1985), p. 38.
- ⁴⁰C. E. Hayes, Ph.D. thesis, Harvard University, 1973.
- ⁴¹H. Wolf, S. Deubler, D. Forkel, H. Foettinger, M. Iwatschenko-Borho, F. Meyer, M. Renn, and W. Witthuhn, 14th International Conference on Defects in Semiconductors, Paris, France, 1986 (unpublished).
- ⁴²F. Meyer, S. Deubler, H. Plank, W. Witthuhn, and H. Wolf, 7th International Conference on Hyperfine Interactions, Bangalore, India, 1986 (unpublished).
- ⁴³F. D. de Wette, *Phys. Rev.* **123**, 103 (1961).